

ZMP stabilization of Rapid Mobile Manipulator

Dongil Choi, Jun-ho Oh, *Member, IEEE*

Abstract—This paper introduces a motion planning method for a rapid mobile manipulator using an inverted pendulum model. We design a linear quadratic optimal controller to stabilize ZMP. The two kinds of ZMP stabilization strategies (*Fixed ZMP* and *Relaxed ZMP*) are proposed. The highly geared manipulator is controlled by a Cartesian computed torque (*CCT*) control for compliant motion. A rapid mobile manipulator called KDMR-1 has been developed for its application. The high acceleration and speed performances of the proposed methods are shown by a rapid maneuvering experiment.

I. INTRODUCTION

MOST mobile manipulators have quite a low level of acceleration performance in spite of the wheel driving system, because the mobile manipulator is basically unstable.

Stabilization of mobile manipulator is a topic that has been widely studied. Dubowsky [1] and Fukuda [2] considered stabilization methods for a stationary vehicle using the conventional optimal time trajectory planning of a manipulator. Sugano [3] used the ZMP (Zero-Moment Point [4]) as a stability measurement for planning the trajectory of a redundant manipulator. Papadopoulos [5] used the force-angle (FA) stability measure, which gives a simple geometric interpretation that predicts whether a robot will tip over. Kim [6] proposed a real-time ZMP compensation method using null motion. Alipour [7] used the Moment-Height Stability (MHS) Measure to detect overturning and to maintain stability. Many studies investigated tip-over prevention methods during manipulation. However, there has been no specific research that focused on the high acceleration performance of a mobile manipulator. Furthermore, some of researches are limited to a simulation due to the complexity of its algorithm and the lack of computational power.

The motion planning using an inverted pendulum model is simple but widely used method. Kajita [8] designed a walking pattern using the inverted pendulum model with preview controller to stabilize ZMP. His walking pattern algorithm is adapted to HRP-2. Sugihara [9] used the inverted pendulum model for a real-time walking pattern

generation. Also, Park [10] designed a real-time walking pattern using the ZMP equation of simple inverted pendulum model and this walking pattern was implemented on KHR-3 (HUBO). The strength of the motion planning method using the inverted pendulum model is simple enough to apply the real-time system and also guarantees the ZMP stability. We apply the motion planning method using the inverted pendulum model to a rapid mobile manipulator.

In our previous research [11], we proposed the ZMP stabilization method of a four-wheel mobile platform for high acceleration performance using an inverted pendulum model. We achieved the maximum acceleration 0.5 g and maximum velocity 20 km/hr in spite of the high CoM (center of mass). In this paper, we design controllers to stabilize the ZMP of the inverted pendulum models as two different strategies. One is a *fixed* ZMP strategy and the other is *relaxed* ZMP strategy. The motion trajectory for 5-DOF (degree of freedom) manipulator is generated from these inverted pendulum models. We use a Cartesian computed torque (*CCT*) control for compliant control of this manipulator. We can control the 5-DOF manipulator to have difference compliances in Cartesian coordinates.

For its application, we have developed the dynamic mobile manipulator named KDMR-1 (KAIST Dynamic Mobile Robot-1) shown in Fig. 1. An experiment is conducted to evaluate the proposed methods.

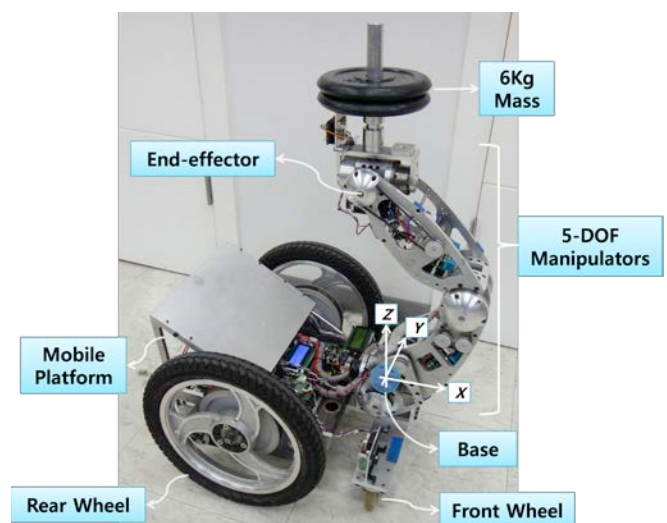


Fig. 1. Dynamic Mobile Manipulator (KDMR-1)

Manuscript received September 28, 2011. This research was supported by the Ministry of Knowledge Economy, Republic of Korea.

D. CHOI is with Humanoid Robot Research Center, KAIST, Daejeon, Republic of Korea (phone: +82-10-7453-1023; fax: +82-42-350-3263; e-mail: doyle.choi.cdi@gmail.com)

J. Oh is with Humanoid Robot Research Center, KAIST, Daejeon, Republic of Korea (email: jhoh@kaist.ac.kr)

II. MODELING

A. 5-DOF Manipulator

The manipulator of KDMR-1 has 5-DOF as shown in Fig. 2. There are three pitch joints, θ_2 , θ_3 , θ_4 and two roll joints, θ_1 , θ_5 . The main purpose of the manipulator is to control the ZMP of the entire system by moving the 6 kg mass on the end-effector. Only for the ZMP control, we just need 2-DOF in the simplest case. One is for the X-axis ZMP and the other is for the Y-axis ZMP. However, we also want to control the height along the Z-axis and the orientation of the end-effector. Therefore we need three more degree of freedoms. The two pitch joints, θ_2 , θ_3 and one roll joints, θ_1 are controlled by CCT control [12, 13] and the orientation of the end-effector, θ_4 , θ_5 is controlled by PD-servo.

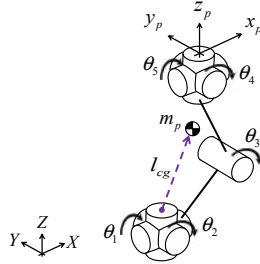


Fig. 2. 5-DOF Manipulator

The reason that we use CCT control is for active suspension like motion. The purpose of a rapid mobile manipulator, KDMR-1 is basically to deliver a small object. We just put an object on the end-effector without any bonding. The rapid mobile manipulator is operated on the normally flat ground. The ground condition is not perfectly good for the rapid mobile manipulator. If we use high gain PD-servo to control the manipulator, some small irregularity on the ground is able to cause critical vibrations on the end-effector of the manipulator. In this case, the small object will be fall down on the ground. For preventing this kind of instability, we can imagine spring and damper elements to reduce vibrations. However, we just use CCT control to accomplish joints compliance without any passive elements. CCT control does not require contact force sensors and only needs electric motors and encoder signals. We can easily obtain different stiffness and damping characteristics on each Cartesian axis independently according to a gain setting.

In the case of the orientation of the end-effector, we simply use PD-servo, because the orientation of the end-effector is not crucial for compliance.

B. Inverted Pendulum Model

The KDMR-1 has two active wheels and two caster wheels as shown in Fig. 1. The front wheels are caster wheels and the rear wheels are active wheels using a differential drive mechanism. The length between front

wheels and rear wheels is 0.3 m. At the end-effector, we put the 6 kg mass to enhance the ZMP compensation effect using the manipulator. The basic posture of the manipulator has a bent shape, as shown in Fig. 1, for a suspension effect and to prevent a singularity. The initial height from base to end-effector is determined as 0.48 m.

In this paper, we deal with the forward movement along the X-axis and the rotational movement on Z-axis of the rapid mobile manipulator. The linearized inverted pendulum model for pitch joints on XZ-plane and roll joints on the YZ-plane are depicted in Fig. 3. We will refer the linearized model for pitch joints as pitch model and the model for roll joints as roll model. By calculating the CoM of the bent-shape mobile manipulator, we simplify the manipulator as a single inverted pendulum, m_p with a length, l and the mobile platform as a single lumped mass, m_c in Fig. 3. To use linearized models, we assume that the centrifugal acceleration due to the X-axis offset from the center of rotation of mobile platform to the origin of the 5-DOF manipulator is ignorable.

The velocity of cart along X-axis is v_x and the inclined angle of the pitch model is ϕ_y . The velocity of cart along Y-axis is v_y and the inclined angle of the roll model is ϕ_x . The force and torque input for the pitch model is f_x , τ_y , respectively and the force and torque inputs for the roll model is f_y , τ_x , respectively.

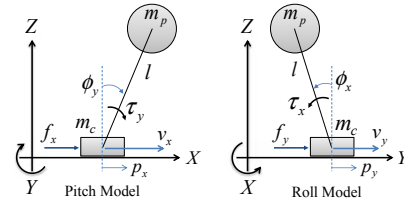


Fig. 3. Inverted Pendulum Model of Pitch Joints and Roll Joints

The linearized equation of motion of the pitch model is derived as follows

$$\begin{cases} \dot{v}_x = -\frac{m_p g}{m_c} \cdot \phi_y + \frac{1}{m_c} \cdot f_x - \frac{1}{m_c l} \tau_y \\ \ddot{\phi}_y = \frac{(m_p + m_c) g}{m_c l} \cdot \phi_y - \frac{1}{m_c l} \cdot f_x + \left(\frac{m_p + m_c}{m_p m_c l^2} \right) \cdot \tau_y \end{cases} \quad (1)$$

The state-space equation of the pitch model becomes as follows

$$\begin{aligned} \dot{x}_x &= A_x x_x + B_x u_x \\ x_x &= [v_x \quad \phi_y \quad \dot{\phi}_y]^T, u_x = \begin{bmatrix} f_x & \tau_y \end{bmatrix}^T \end{aligned} \quad (2)$$

The linearized equation of motion of the roll model is 4 derived as similar forms. The linearized ZMP of the pitch and roll model is as follows

$$p_x = -\frac{\tau_y}{(m_p + m_c)g}, \quad p_y = \frac{\tau_x}{(m_p + m_c)g} \quad (3)$$

The difference of the equation of motion between the pitch model and the roll model is due to the direction of rotation of the inverted pendulum. We can design basically same controllers about both models. Our inverted pendulum model is very similar to one of Kajita's model [8]. The main difference between Kajita's model and our model is the existence of the torque input on the inverted pendulum. On the Kajita's model, there is no torque input for the inverted pendulum. They only used the jerk of CoM of the inverted pendulum as a control input. The inverted pendulum becomes a free rotating system. In this case, the zero-moment point becomes the center of rotation of the inverted pendulum and p_x, p_y maintains always zero.

In our research, however, the inverted pendulum model has two inputs. One is the force on the mobile platform and the other is the torque on the inverted pendulum. To stabilize an inverted pendulum model and the ZMP of the system, we use a state-feedback controller. The state-feedback gain can be found by a linear quadratic optimal control. By changing the weighting matrix, we can tune the non-minimum phase characteristic of the inverted pendulum model as two strategies, fixed and relaxed ZMP. In the next chapter, we present an optimal solution and the simulation results of those feedback controllers.

III. CONTROL SYSTEM DESIGN

A. Cartesian Computed Torque Control for Compliance

The manipulator of KDMR-1 is actuated by electric motors with harmonic gear and pulleys. To control highly geared electric motors, we generally use the PD-servo [14]. In this case, we usually set the high position gain for good tracking performance. In our rapid mobile manipulator, however, we need joint compliance and also good position tracking. To accomplish these requirements, we use CCT control.

The equation of motion of the manipulator is shown as the following equation.

$$\tau = M(\theta) \cdot \ddot{\theta} + V(\theta, \dot{\theta}) + G(\theta) \quad (4)$$

where $\theta, \dot{\theta}$ and $\ddot{\theta} \in R^n$ are joint angle configurations, $\tau \in R^n$ is the joint torque vector, $M(\theta) \in R^{n \times n}$ is an inertia matrix, and $V(\theta, \dot{\theta}) \in R^n$ is the Coriolis and centrifugal torque vector, and $G(\theta) \in R^n$ is the gravity torque vector.

The kinematic relations between the joint space and Cartesian space are expressed as follows [15, 16]

$$X = f(\theta) \quad (5)$$

$$\dot{X} = J(\theta)\dot{\theta} \quad (6)$$

$$\ddot{X} = J(\theta)\ddot{\theta} + \dot{J}(\theta)\dot{\theta} \quad (7)$$

where $X \in R^m$ is the Cartesian vector representing position of the end-effector and $J \in R^{m \times n}$ is the Jacobian matrix.

In our system, the Cartesian vector X is the position coordinates of the end-effector as follows.

$$X = [x_p \quad y_p \quad z_p]^T \quad (8)$$

We control two pitch joints, θ_2, θ_3 and one roll joints, θ_1 using CCT control. The number of joints, n is three and also the number of the Cartesian vector, m is three. Therefore the Jacobian matrix is a square matrix. The joint space acceleration vector leads to

$$\ddot{\theta} = J^{-1}(\theta) \{ \ddot{X} - \dot{J}(\theta)\dot{\theta} \} \quad (9)$$

The computed Cartesian space acceleration vector is represented with a feedback control scheme as follows.

$$\ddot{X}_{cp} = \ddot{X}_d + K_v(\dot{X}_d - \dot{X}) + K_p(X_d - X) \quad (10)$$

where $\ddot{X}_d, \dot{X}_d, X_d$ is the desired Cartesian space acceleration, velocity and position vector, respectively and K_p, K_v are the position and velocity gain of the CCT control, respectively. Using equation (9) and (10), the computed joint space acceleration vector becomes

$$\ddot{\theta}_{cp} = J^{-1}(\theta) \{ \ddot{X}_{cp} - \dot{J}(\theta)\dot{\theta} \} \quad (11)$$

Using equation (4) and (11), the computed joint space torque required to achieve the computed Cartesian space acceleration is represented as

$$\tau_{cp} = \hat{M}(\theta) \cdot \ddot{\theta}_{cp} + \hat{V}(\theta, \dot{\theta}) + \hat{G}(\theta) \quad (12)$$

where τ_{cp} is the computed joint space torque vector and $\hat{M}(\theta), \hat{V}(\theta, \dot{\theta}), \hat{G}(\theta)$ are the inertia matrix of the model, the Coriolis and centrifugal torque vector of the model, the gravity torque vector of the model, respectively.

The error dynamics is as follows

$$0 = \hat{M} \cdot J^{-1} \{ \ddot{X}_{cp} - (J\ddot{\theta} + \dot{J}\dot{\theta}) \} + (\hat{M} - M)\ddot{\theta} + (\hat{V} - V) + (\hat{G} - G) \quad (13)$$

Under the assumption that the model and actual system is

quite well matched, the error dynamics become simple as follows [13]

$$\hat{M}-M ; 0, \hat{V}-V ; 0, \hat{G}-G ; 0 \quad (14)$$

$$\ddot{E}+K_v \dot{E}+K_p E=0 \quad (15)$$

where $E=X_d-X$. CCT control scheme is depicted in Fig. 4.

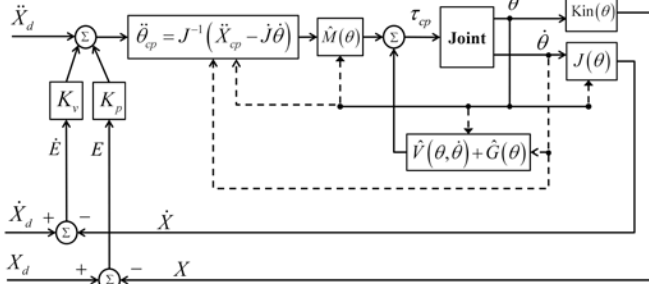


Fig. 4. Cartesian Computed Torque (CCT) Control Scheme

The pole of the error dynamics equation (15) is as follows

$$s = \frac{-K_v \pm \sqrt{K_v^2 - 4K_p}}{2} \quad (16)$$

The relationship between the feedback gain K_p , K_v and the motion characteristic of the manipulator is as follows

- i) $K_v^2 = 4K_p \rightarrow$ Critically damped
- ii) $K_v^2 > 4K_p \rightarrow$ Over-damped
- iii) $K_v^2 < 4K_p \rightarrow$ Under-damped

Even in a low position gain, CCT control provides quite good position control performance maintaining joint compliance rather than PD-servo, because the torque computed from CCT control compensates for the gravity and nonlinear torque terms. In the actual system, we choose under-damped feedback gains for suspension-like motion as $K_p = 30$, $K_v = 8$ on the Y-axis and as $K_p = 30$, $K_v = 7$ on the Z-axis. By choosing a low position gain and corresponding velocity gain, we can achieve suitable compliance of the manipulator and small amount of position error compared to low gain PD-servo. On the X-axis, we set comparably high position feedback gain as $K_p = 200$, $K_v = 20$ for more accurate ZMP trajectory following.

By using CCT control, we set the different feedback gain on each axis. We tune the high feedback gain on X-axis for good position tracking performance and the low feedback gain on the Y, Z-axis for suspension-like motion. This is the strength of CCT control compared to the joint space computed torque control and usual PD-servo controller.

In the actual system, KDMR-1, the computed joint space torque is converted to the voltage of electric motor considering the motor dynamics equation as

$$V_i = \frac{Rm_i}{n_i K_i^T} (\tau_{cp,i} + Jm_i \ddot{\theta}_i + Bm_i \dot{\theta}_i) \quad (17)$$

where $V_i \in R^n$ is the voltage of the i th joint, n_i is total gear ratio of the i th joint, K_i^T is the torque constant of the i th motor, Rm_i is the terminal resistance of the i th motor, $\tau_{cp,i}$ is the computed joint space torque of the i th joint, Jm_i is the output inertia of motor, harmonic gear and pulley assembly of the i th joint and Bm_i is the output viscous friction coefficient of the motor, harmonic gear and pulley assembly of the i th joint. We apply the voltage to each joint as a PWM (Pulse-width Modulation) signal. Table 1 shows the important values of the mechanical parameters of the KDMR-1.

TABLE 1
PARAMETERS OF 5-DOF MANIPULATOR

	Joint 1	Joint 2	Joint 3	Joint 4	Joint 5
n_i	296.3	190	120	187.5	181.3
Jm_i (Nm · s ²)	2.91	1.26	0.71	0.83	0.79
Bm_i (Nm · s)	162.6	84.92	75.24	76.72	71.70
I_i (Nm · s ²)	0.02	0.02	0.024	0.06	0.06
m_i (kg)	8	8	4.8	8.5	8.5
l_i (m)	0.3	0.3	0.3	0.15	0.15

where I_i is the link inertia of the i th joint, m_i is the link mass of the i th joint, l_i is the link length of the i th joint. Because of the high gear ratio, the output inertia of motor, harmonic gear and pulley assembly is much bigger than the link inertia and the output viscous friction is not ignorable.

B. ZMP Stabilization Control Using State-feedback

The target system researched in this paper has a four-wheel driving system. It has a support polygon on a two-dimensional space through connections of four points on the ground. If the ZMP is located inside the support polygon, the system is secure in terms of its stability [4, 6, 17]. Otherwise, the system starts to roll over.

We design the state-feedback controller gain, K to minimize the quadratic cost function, J .

$$u = K(x_d - x) \quad (18)$$

$$J = \int_0^\infty (x^T Q x + u^T R u) dt \quad (19)$$

where $x_d = [v_j^{des} \ 0 \ 0]^T$, $j = x, y$. The Q is the weighting matrix for the state and R is the weighting matrix for control inputs. The associated Riccati equation is

$$0 = A^T S + SA - SB \cdot R^{-1} \cdot B^T S + Q \quad (20)$$

By using the solution of Riccati equation, S , we can get the optimal feedback gain, K as

$$K = R^{-1} B^T S \quad (21)$$

We simulate the state-feedback controller in Fig. 5 by changing the weighting matrices. In the model 1, we set the weighting matrices as

$$Q = \begin{bmatrix} 1 & 0 & 0 \\ 0 & 0 & 0 \\ 0 & 0 & 0 \end{bmatrix}, R = \begin{bmatrix} 3 \times 10^{-5} & 0 \\ 0 & 10^2 \end{bmatrix} \quad (22)$$

In the model 1, we apply a desired velocity, v_x^{des} as 3.5 m/sec (12.6 km/hr) at 1 sec. We can find an undershoot on the velocity graph. We will refer this undershoot as a *reverse action*. Basically this is a non-minimum phase characteristic of the inverted pendulum due to a right-half plane zero. Actually this kind of undershoot is undesirable in usual system because it makes a big tracking error in transient state. To overcome this problem, Kajita [8] used a preview control and Napoleon [18] used two masses inverted pendulum model. In our research, however, we accept this reverse action. Because, there is a positive effect to push forward the inverted pendulum more quickly by moving the mobile platform backward. The fixed ZMP strategy makes the system to accelerate more dynamically. We can observe the maximum acceleration is about 0.7 g and the maximum velocity is 3.5 m/sec (12.6 km/hr).

The ZMP p_x is normalized from -1 to 1. Here, '0' indicates that the ZMP is located at the center of the support polygon, and '1' or '-1' signifies that the ZMP is located on the edge of the support polygon. The weighting about force input is much smaller than one of the torque input. It means that the feedback gain minimizes much more on the torque input. Resultingly, the force input is dominant. The torque input is almost zero in the model 1. It means that the ZMP coincides with the center of rotation of the inverted pendulum. To maintain the ZMP on the center of rotation of the inverted pendulum, the reverse action is inevitable.

In model 2, we set the weighting matrices as

$$Q = \begin{bmatrix} 1 & 0 & 0 \\ 0 & 0 & 0 \\ 0 & 0 & 0 \end{bmatrix}, R = \begin{bmatrix} 10^{-5} & 0 \\ 0 & 10^{-5} \end{bmatrix} \quad (23)$$

We apply a desired velocity as 1 m/sec at 1sec. The ZMP p_y does not maintain zero and the inverted pendulum rotates opposite direction compared to the model 1. The weighting of the force input is same as the one of the torque input in the model 2. As a result, both the force input and the torque input are valid for controlling the inverted pendulum model. Due to the torque input, we can track the desired

velocity without the reverse action. If the ZMP is located inside of the support polygon, the stability of the system is guaranteed. In this control strategy, we just allow the change of the ZMP inside the support polygon. We will refer this kind of ZMP stabilizing strategy as a *relaxed ZMP strategy*.

The span from front wheels to rear wheels is 0.3m. The span from a left wheel to a right wheel is 0.5m. The model 1 is suitable for the pitch model, because it has a short span and it is required a rapid and dynamic acceleration performance. The model 2 is suitable for the roll model, because the stable area of the ZMP is large enough to apply relaxed ZMP strategy and it provides a good controllability.

Two pitch joints, θ_2, θ_3 and one roll joints, θ_1 are controlled by CCT control to follow the motion generated model 1 and 2. In the next chapter, an experiment is conducted to evaluate control schemes.

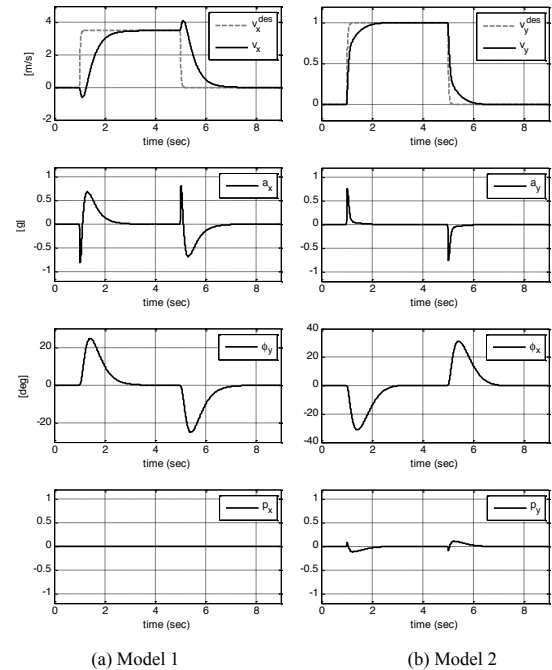


Fig. 5. Simulation results depending on weighting matrices

IV. EXPERIMENTS

A. Rapid Maneuvering Experiment

We carry out a rapid maneuvering experiment using KDMR-1. We present the forward movement on the left side and the rotational movement on the right side in Fig. 6. The dash line is a model value and the solid line is an actual value of the mobile platform.

On the left side, the desired forward velocity is 3.6 m/s (13 km/hr). We can observe that the actual velocity is well controlled by the desired value with the reverse action. The position of the end-effector along X-axis tracks the desired value quite precisely due to the comparably high gain on CCT control. The vibration on deceleration period is due to slips between the ground and tire. The maximum forward acceleration ignoring the vibration is 0.77 g.

On the right side, the desired rotational velocity is 0.8 m/s. The actual rotational velocity tracks the desired value without reverse action. There are tracking errors on the end-effector along Y-axis because the gain of CCT controller on Y-axis is low. Nevertheless, the low gain is good for suspension like motion and makes the end-effector more flexible.

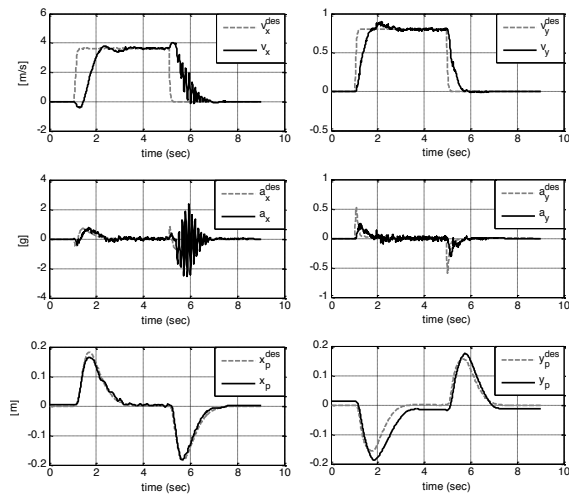


Fig. 6. Rapid Maneuvering Test to Forward Direction

V. CONCLUSION

In this research, we considered a rapid mobile manipulator that has high acceleration and speed mobility as maximum 13 km/hr and 0.77 g. The 5-DOF manipulator was controlled by Cartesian computed torque control to have difference compliances in Cartesian coordinates. The motion trajectories were generated by inverted pendulum models. The ZMP stabilization control was addressed as a linear quadratic optimal control problem. Two kind of ZMP stabilization strategies, fixed and relaxed ZMP were introduced. Experimental results showed the performance of overall control scheme.

REFERENCES

- [1] S. Dubowsky and E. E. Vance, "Planning Mobile Manipulator Motions Considering Vehicle Dynamic Stability Constraints," in *Proc. IEEE Int. Conf. on Robotics and Automation*, pp. 1271-1276, 1987.
- [2] T. Fukuda and Y. Fujisawa, "Manipulator/Vehicle System for Man-Robot Cooperation," in *Proc. IEEE Int. Conf. on Robotics and Automation*, pp. 74-79, 1992.
- [3] Q. Huang, "Coordinated Motion Planning for a Mobile Manipulator considering Stability and Manipulation," *The International Journal of Robotics Research*, vol. 19, pp. 732-742, 2000.
- [4] M. Vukobratovic and B. Borovac, "ZERO-MOMENT POINT — THIRTY FIVE YEARS OF ITS LIFE," *International Journal of Humanoid Robotics*, vol. 1, pp. 157-173, 2004.
- [5] E. Papadopoulos and D. Rey, "The Force-Angle Measure of Tipover Stability Margin for Mobile Manipulators," *Vehicle System Dynamics*, vol. 33, pp. 29-48, 2000.
- [6] J. Kim, et al., "Real-time ZMP Compensation Method using Null Motion for Mobile Manipulators," in *Proc. IEEE Int. Conf. on Robotics and Automation*, pp. 1967-1972, 2002.

- [7] S. A. A. Moosavian and K. Alipour, "Tip-Over Stability of Suspended Wheeled Mobile Robots," in *Proc. IEEE Int. Conf. on Mechatronics and Automation*, pp. 1356-1361, 2007.
- [8] S. KAJITA, et al., "Biped Walking Pattern Generation by using Preview Control of Zero-Moment Point," in *Proc. IEEE Int. Conf. on Robotics and Automation*, Taipei, Taiwan, pp. 1620-1626, September 14-19, 2003.
- [9] T. Sugihara, et al., "Realtime Humanoid Motion Generation through ZMP Manipulation based on Inverted Pendulum Control," in *Proc. IEEE Int. Conf. on Robotics and Automation*, Washington, DC, pp. 1404-1409, May, 2002.
- [10] I.-W. Park, et al., "Online Walking Pattern Generation and Its Application to a Biped Humanoid Robot — KHR-3 (HUBO)," *Advanced Robotics*, vol. 22, pp. 159-190, 2008.
- [11] M. Kim, et al., "Stabilization of a Rapid Four-wheeled Mobile Platform Using the ZMP Stabilization Method," in *Proc. IEEE/ASME International Conference on Advanced Intelligent Mechatronics*, Montreal, Canada, pp. 317-322, July 6-9, 2010.
- [12] D. Bevely, et al., "A Simplified Cartesian-Computed Torque Controller for Highly Geared Systems and Its Application to an Experimental Climbing Robot," *Journal of Dynamic Systems, Measurement, and Control*, vol. 122, pp. 27-32, 2000.
- [13] J. H. Park and K. D. Kim, "Biped robot walking using gravity-compensated inverted pendulum mode and computed torque control," in *Proc. IEEE Int. Conf. on Robotics and Automation*, Leuven, Belgium, pp. 3528-3533, 1998.
- [14] I. W. Park, et al., "Development of Humanoid Robot Platform KHR-2 (KAIST Humanoid Robot-2)," in *IEEE-RAS International Conference on Humanoid Robots*, pp. 292-310, 2004.
- [15] A. Liegeois, "Automatic Supervisory Control of the Configuration and Behavior of Multibody Mechanisms," in *IEEE Transactions On Systems, Man, and Cybernetics*, pp. 868-871, 1977.
- [16] Y. Nakamura, et al., "Task-Priority Based Redundancy Control of Robot Manipulators," *The International Journal of Robotics Research*, vol. 6, pp. 3-15, 1987.
- [17] S. Sugano, et al., "Stability Criteria in Controlling Mobile Robotics Systems," in *Proc. IEEE Int. Conf. on Intelligent Robots and Systems*, pp. 832-838, 1993.
- [18] Napoleon, et al., "Balance Control Analysis of Humanoid Robot based on ZMP Feedback Control," in *Proc. IEEE Int. Conf. on Intelligent Robots and Systems*, EPFL, Lausanne, Switzerland, pp. 2437-2442, October, 2002.